

Quantitative *in Situ* Hybridization to Measure Single-Cell Changes in Vasopressin and Oxytocin mRNA Levels After Osmotic Stimulation

Joseph T. McCabe,^{1,4} Mitsuhiro Kawata,² Yutaka Sano,²
Donald W. Pfaff,¹ and Robert A. Desharnais³

Received June 12, 1989; accepted August 11, 1989

KEY WORDS: autoradiography; morphometry; biological models; *in situ* hybridization; neurohypophysial system; supraoptic nucleus; vasopressin; oxytocin; messenger RNA.

SUMMARY

1. The measurement of cellular mRNA content by quantitative *in situ* hybridization is a valuable approach to the study of gene expression in brain since this tissue exhibits a high degree of phenotypic heterogeneity.

2. The cellular content of vasopressin and oxytocin mRNA in hypothalamo-neurohypophysial system neurons was altered by maintaining rats for 24 hr on 2% sodium chloride water.

3. Statistical and graphical techniques were then used to analyze cell by cell how mRNA levels were altered as a result of osmotic stimulation. We propose that the negative binomial probability distribution is a suitable model to describe how mRNA content varies across a defined cell population. For both measures of oxytocin and vasopressin mRNA levels, maximum-likelihood estimation indicated that this model adequately described empirical findings obtained from rats drinking tap water or salt water.

¹Neurobiology & Behavior Laboratory, The Rockefeller University, New York, New York 10021-6399.

²Department of Anatomy, Kyoto Prefectural University School of Medicine, Kawaramachi-Hirokoji, Kamikyo-ku, Kyoto 602, Japan.

³Department of Biology, California State University, Los Angeles, California 90032.

⁴To whom correspondence should be addressed at Department of Anatomy, Uniformed Services University of the Health Sciences, Department of Defense, 4301 Jones Bridge Road, Bethesda, Maryland 20814-4799.

4. Both graphical and statistical analyses suggested how the defined neural system responds to osmotic stimulation: mRNA content was altered as a multiplicative function of "initial state." The utility and limitations of the quantitative approach are discussed.

INTRODUCTION

In situ hybridization allows one to identify cells that contain a particular messenger ribonucleic acid (mRNA). A probe, applied to the tissue section, forms double-stranded hybrid molecules through base complementation with the mRNA of interest. The reporter component of the probe (an isotope, an enzyme substrate, a fluorescent marker, or an antigenically recognizable molecule) identifies those cells which contain the hybridized mRNA. Under optimized conditions, one can use the amount of reporter substance present in the cytoplasm of each labeled cell as an indicator of that cell's quantity of the particular mRNA. Carefully applied methodology further allows tissue samples from different experimental treatments to be directly compared. We, and others, have recently discussed at length the issues surrounding quantitative approaches to *in situ* hybridization (Lewis *et al.*, 1989; McCabe *et al.*, 1989b,c; Uhl, 1989; Young, 1989), and we have recently proposed graphical and statistical procedures that are useful for data summarization and analysis (McCabe *et al.*, 1989).

The application of graphical analytic methods allow the investigator immediately to comprehend patterns or general trends in single data sets or across data sets derived from experimental treatments. Quantile plotting provides one graphical procedure for summarizing individual elements of a data set (Chambers *et al.*, 1983; Wilk and Gnanadesikan, 1968). To generate a quantile plot, the raw data, the measured quantity of mRNA per cell (in the present case, autoradiography grain density) from the anatomical area of interest, are listed in rank order from the smallest to the largest value in the data set. One then plots each value by its rank order. To compare two data sets, the quantile distributions of both data sets are separately generated, and the correspondingly paired (ranked) quantile values from each data set are plotted, respectively, on the *x* and *y* axes (see Procedures).

Graphical analysis is complemented by statistical estimation and hypothesis testing. We have recently employed a statistical model which can account for variation in grain density over both labeled and unlabeled cells (McCabe *et al.*, 1989). This two-component statistical model can account for the inherent phenotypic heterogeneity of neural tissue where one observes (1) a low degree of grain density over unlabeled cells and (2) variation in grain density over labeled cells. Grain density over unlabeled cells ("background") arises from the random disintegration of isotope over a relatively uniform field. Hence, this variation is suitably described as a Poisson process (England and Rogers, 1970). Over labeled cells, however, grain density is the result of random uniform disintegration processes as well as from variation that arises from the fact that each cell is a distinct, discrete, and independent element of the target population. The latter

combination of variation gives rise to a negative binomial distribution (McCabe *et al.*, 1989). The present report will examine the suitability of the negative binomial as a model of mRNA variation within a defined cell population, in this case a population composed of labeled neurons only.

It should be noted at the outset that we believe the negative binomial distribution may be suitable only for data that are derived from a cell population which exhibits no change in cell size across experimental treatment groups. If cell size is altered by experimental treatment, as it is for hypothalamic neurosecretory neurons when rats drink salt water (Kawata *et al.*, 1988a), then the data should be expressed in terms of grain density (grains per cell divided by cell profile area).

The graphical and statistical analyses are explicated with data derived from *in situ* hybridization to detect vasopressin and oxytocin mRNA (Kawata *et al.*, 1988c). When rats are given salt water to drink in place of tap water, many investigations have observed increased amounts of vasopressin and oxytocin mRNA in hypothalamic magnocellular neurons of the supraoptic and paraventricular nuclei (e.g., Hyodo *et al.*, 1988; Lightman and Young, 1987; McCabe *et al.*, 1986c; Sherman *et al.*, 1986; Van Tol *et al.*, 1987). *In situ* hybridization with tritium-labeled oligomers complementary to oxytocin and vasopressin mRNA were used to measure changes in supraoptic nucleus cellular mRNA content following salt drinking.

METHODS

Tissue Preparation and Hybridization

Ovariectomized rats (Sprague-Dawley, 200-g body weight) were housed in single cages with free access to food. Animals ($n = 2$ per group) were given tap water or 2% NaCl water to drink for 1, 4, or 14 days before they were sacrificed. Following administration of anesthesia (sodium pentobarbital) each rat was perfused via the left cardiac ventricle with 100 ml of physiological saline and then 300–500 ml of 4% paraformaldehyde in 100 mM phosphate buffer (pH 7.6). The brains were then removed from the calvarium, blocked with a razor blade, postfixed in the same fixative (1 hr, 4°C), and then immersed in 2% sucrose, 100 mM phosphate buffer (24 hr, 4°C). Frozen blocks of hypothalamic tissue were sectioned (6 μm) in the coronal plane and tissue samples containing supraoptic nucleus tissue were mounted on gelatin-coated slides. The tissue was then fixed and processed for *in situ* hybridization as previously described (Kawata *et al.*, 1988a; McCabe *et al.*, 1986a; McCabe and Pfaff, 1989). Autoradiograms were prepared by dipping in Kodak NTB-3 and exposures were for 4 weeks at 4°C.

The gene sequences encoding oxytocin and vasopressin mRNA exhibit a high degree of homology (Ivell and Richter, 1984). Oligonucleotide probes that are complementary to these gene products must be carefully selected so as to minimize potential cross-hybridization (for discussion see Kawata *et al.*, 1988b). Probes were therefore prepared from the 3' end of the genes where mRNA transcript homology is minimal. The oxytocin probe was a 25 mer (3'-

GCTGGGACTCAGACGGAAGAGGCTC-5') from base pairs 912 to base pair 936 of the oxytocin gene (Ivell and Richter, 1984). The vasopressin probe was a 26 mer (3'-TCGACCTGCCCGGTCGGGCCCTCGAC-5'), bases 1843-1868 of the vasopressin gene (Schmale *et al.*, 1984). The procedure for labeling the oligomers has been described previously (Kawata *et al.*, 1988b). In brief, the oligomers were end-labeled with [1',2',5'-³H]deoxycytidine triphosphate (Amersham TRK.625) by utilizing terminal deoxynucleotidyl transferase (Bethesda Research Laboratories). Probes were then purified by passage through a NENSORB cartridge (DuPont, Wilmington, DE).

Data Collection

In our previous study (McCabe *et al.*, 1989), we analyzed grain counts from both labeled and unlabeled neurons of the supraoptic nucleus by counting grains over all cell profiles. This was to examine the suitability of the two-component statistical model as an example of measures of an anatomically defined brain site which is comprised of labeled and unlabeled neurons. Here we have categorized cells as either vasopressinergic or oxytocinergic before grain counting to analyze phenotypically homogeneous samples. Oxytocin- and vasopressin-containing cells of the supraoptic nucleus are anatomically segregated (Defendini and Zimmerman, 1978; Hou-Yu *et al.*, 1986; Kawata, 1983; Rhodes *et al.*, 1981; Vandesande and Dierickx, 1975). In general, the dorsal one-third aspect and the ventral one-third aspect of this nucleus are comprised of oxytocinergic and vasopressinergic cells, respectively. Coronal sections through the supraoptic nucleus were selected from each of the eight animals (Kawata *et al.*, 1988c). The grains overlying each cell in the dorsal one-third (oxytocin study) or ventral one-third (vasopressin study) aspects of the supraoptic nucleus were counted by utilizing the image analysis system described by Takamatsu and co-workers (1986). The grains overlying individual cell profiles were digitized as pixels per cell profile. Estimates of background, grain density over neuropil the same area as neuronal profiles, were invariably fewer than 5 pixels/profile area.

Data Analysis

Histograms were generated to summarize the data from each treatment condition, where the number of cells (ordinate axis) was plotted against the measure of grain counts per cell (pixels per cell profile). Close visual inspection of the data sets (see Kawata *et al.*, 1988c, Fig. 4) suggested that data from rats maintained on salt water for either 4 or 14 days were not appropriate for the current analysis. These data sets were multimodal and would therefore require applying a more complex, mixed statistical model (see McCabe *et al.*, 1989). In addition, cell profile areas were not measured, and this makes the data obtained from rats on salt water for 4 or 14 days unsuitable for comparison, in the present context, to the data obtained from rats maintained on tap water. It is known that salt loading for 4 or 14 days drastically increases the cellular volume of supraoptic nucleus neurons (Kawata *et al.*, 1988a). To make comparisons across tissue samples with widely different cell sizes requires one to take this change into

account by using, for example, measures of grain density (McCabe *et al.*, 1986b; Przybylski, 1970). Hence, *for clarity and instructive purposes* we restrict the analysis to data obtained from the control and 1-day salt drinking rats.

The data were represented in the following quantile plots: (1) *empirical quantile plots*, where data of each group were plotted against each datum's fraction value (see below); (2) *quantile-quantile plots*, to compare directly the data of control and salt-treated animals, and (3) *residual quantile plots*, to analyze the basis for differences between treatment conditions. The quantile distributions of each data set were formed by ranking the data from smallest to largest value. Each datum's fraction value was computed using the formula, $(i - 0.5)/n$, where i indicates the datum's rank, and n represents the number of elements in the data set. Empirical quantile plots and quantile-quantile plots were then produced utilizing the equivalent (or interpolated) quantiles. Residual quantile plots were produced by calculating the residuals, differences between the quantiles of equivalent fraction values, for each data set obtained from salt drinking rats minus the control (tap-water drinking) group.

A modification of the procedure recently described (McCabe *et al.*, 1989) was employed for statistical estimation. Since only subregions of the supraoptic nucleus were analyzed, the case for a mixed population model, to account for labeled and unlabeled cells was circumvented. A single-component statistical model, the negative binomial distribution, was directly applied to each data set.

Let x represent the number of pixels per cell. The probability of observing x pixels in a cell is given by the negative binomial distribution

$$b(x) = \binom{\alpha + 1 - x}{\alpha - 1} \beta^x (1 - \beta)^{-\alpha - x}, \quad x = 0, 1, 2, \dots,$$

where

$$\binom{\alpha + 1 - x}{\alpha - 1} = \frac{\alpha(\alpha + 1)(\alpha + 2) \cdots (\alpha + x - 1)}{x!}.$$

The parameters of the negative binomial, α and β , represent "shape" and "scale" parameters for the underlying probability distribution of cell mRNA content (McCabe *et al.*, 1989). Small values of α indicate a positively skewed distribution (heavy right tail), whereas large values suggest a normal distribution. The mean of the negative binomial is given by $\alpha\beta$ and the variance by $\alpha\beta(\beta + 1)$.

The parameters of the negative binomial were estimated using the method of maximum likelihood. Let $y(x)$ equal the observed number of cells containing x pixels. The maximum-likelihood estimates are the values of α and β which maximize the log-likelihood function

$$\log L = \sum_{x=0}^m y(x) \log b(x).$$

In practice, this function is maximized by setting the first partial derivatives with respect to α and β equal to zero. The second partial derivative, evaluated using the maximum-likelihood estimates, provide a variance-covariance matrix for α and β . This matrix can be used to obtain standard errors and confidence intervals

and to test statistical hypotheses. Furthermore, an estimate and standard deviation can be obtained for any differentiable function of α and β using the method of Taylor expansion (Kendall and Stuart, 1977). Formulas for the first and second derivatives of the log-likelihood function, the variance-covariance matrix, confidence intervals, and Taylor expansions can be obtained from the previously published two-component statistical model (McCabe *et al.*, 1989) by simply setting the parameter ϕ in the two-component model equal to zero.

RESULTS

Graphical Analysis

Separate tissue samples of the supraoptic nucleus from animals drinking tap water or 2% NaCl water for 1 day were hybridized with the oligomer probes complementary to a portion of vasopressin mRNA or oxytocin mRNA. Pixel counts, as a measure of autoradiography grains, over vasopressin cells in the ventral portion of the supraoptic nucleus are summarized in Fig. 1 (a and c). Pixel counts from tissue samples that were hybridized with the oligonucleotide probe complementary to oxytocin mRNA are also summarized for counts determined

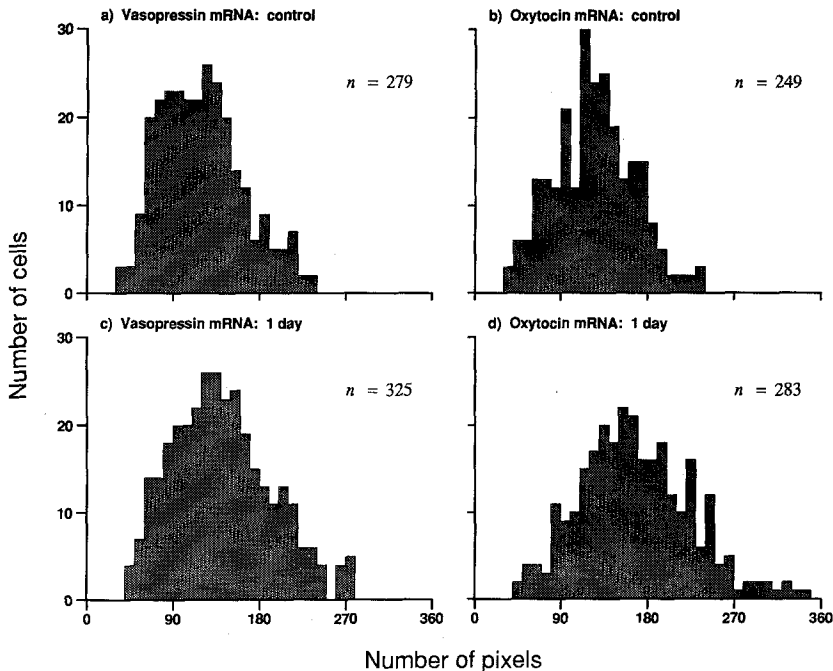


Fig. 1. Frequency histograms of pixel counts for vasopressinergic and oxytocinergic neurons from control rats (a, b) and rats maintained on 2% NaCl for 1 day (c, d). There is slight increase in the amount of labeled vasopressin mRNA for the 1-day treatment (c) relative to the control (a). A more noticeable increase in the amount of labeled mRNA is exhibited by the oxytocinergic cells (b *vs* d). *n* represents the number of sampled cells.

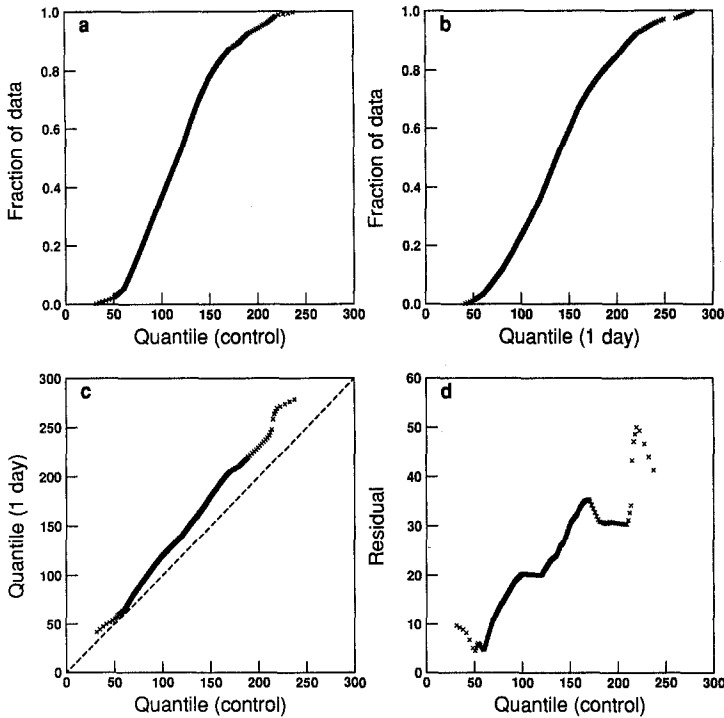


Fig. 2. Quantile plots of vasopressin mRNA data from Fig. 1. (a) Quantile plot of the data from the control rats. (b) Quantile plot of the data from the rats maintained on 2% NaCl for 1 day. (c) Quantile-quantile (Q-Q) plot of the control *vs* 1-day treatments. (d) The residual quantile plot. The dashed line in the Q-Q plot represents the predicted relationship if both data sets were from identical distributions (no treatment effect). The residual quantile plot represents deviations from this dashed line. The Q-Q and residual quantile plots suggest that vasopressin mRNA increases proportionally across the cell population.

over dorsally positioned supraoptic nucleus neurons (Figs. 1b and d). Across treatment conditions, the histograms exhibit a small but detectable change in their overall shape as a result of salt loading: a greater proportion of cells exhibited higher pixel values relative to the control rats maintained on tap water (Figs. 1a and b). Figures 2 (vasopressin mRNA) and 3 (oxytocin mRNA) summarize the same data in terms of empirical quantile plots (a and b). Recall that the quantile plot is a visual summary of the data from each treatment group arranged in ranked form and plotted against the quantile's fraction value. Upon close inspection of Figs. 2 and 3 (a and b), it can be seen that the position of the quantiles of the two data sets do not occupy the same region of the plot as the control data sets. This implies an alteration in the distribution of pixel values across the treatment conditions.

In Figs. 2c and 3c, quantile-quantile (Q-Q) plots are presented for visual comparison of the quantile distributions of each experimentally treated group's data relative to the control (tap water-drinking) group. The Q-Q plots would

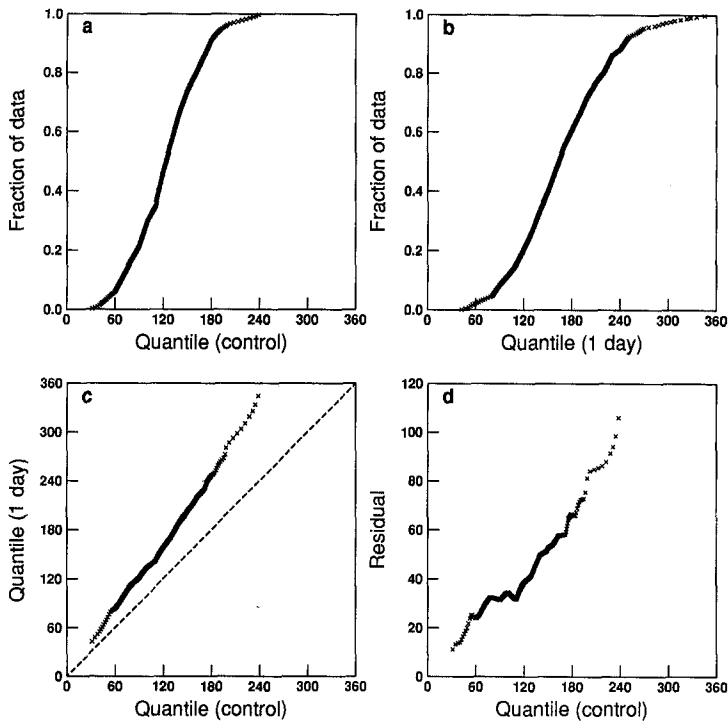


Fig. 3. Quantile plots of oxytocin mRNA data from Fig. 1. The plots in this figure are analogous to those in Fig. 2. The Q-Q and residual quantile plots suggest that oxytocin mRNA also increases proportionally across the cell population.

exhibit slopes of 1 (dashed line) if there was no difference between the control and the salt-drinking groups. In each case the slopes are greater than 1 [approximately 1.18 for the vasopressin quantile data set (Fig. 2c) and about 1.35 for the oxytocin data set (Fig. 3c)]. The residual quantile plots (Figs. 2d and 3d) provide a clear illustration of the differences between the quantile data sets from the control animals compared to those from the salt-loaded animals. If there were no group differences, the residual plots would exhibit slopes and y intercepts equal to zero. If the difference was due simply to an additive increase in mRNA for each cell, the residual quantile would exhibit a slope of zero and a y intercept equal to the additive constant. On the other hand, if each cell increased its mRNA production in proportion to its production prior to osmotic stimulation, then the difference would be multiplicative, and the residual quantile plot would exhibit a linear relation with a positive slope which passes through the origin. In each case the slopes are not equal to zero and the y intercepts are zero (Figs. 2d and 3d), which implies the multiplicative hypothesis.

Statistical Analysis

The method of maximum likelihood was applied to the four data sets to estimate the parameters, α and β . A "goodness-of-fit" χ^2 test was used to assess

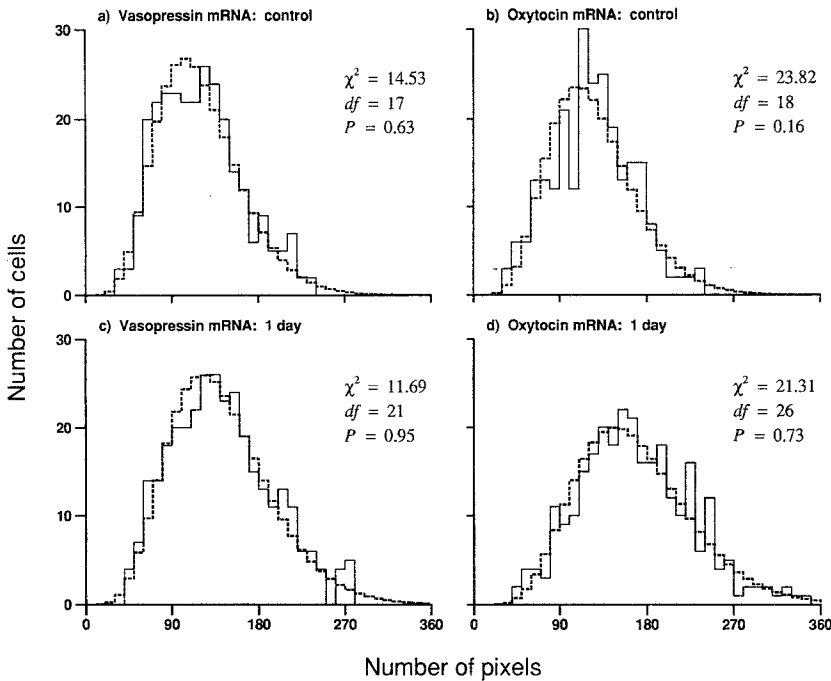


Fig. 4. The observed frequency histograms from Fig. 1. (solid lines) are compared to the expected frequency counts (dashed lines) from the negative binomial distribution. There is a good agreement between the observed and the theoretical distributions. The chi-square test statistic (χ^2), degrees of freedom (df), and probability levels (P) are given for the goodness-of-fit tests. P represents the probability of obtaining a larger χ^2 value due to random chance alone. Values of $P < 0.05$ would result in a rejection of the negative binomial model.

the applicability of the negative binomial function by comparing the expected values determined by $nb(x)$ to the empirically derived (“observed”) data $y(x)$. The goodness-of-fit test failed to reject the model ($P > 0.05$) in each case. A graphical summary of the expected distributions from parameter estimation for the control and 1-day salt-loaded data sets is illustrated in Fig. 4. The dashed line closely follows the histograms of the empirical data sets, suggesting that the negative binomial distribution adequately represents the observed data.

The parameters α and β are of intrinsic interest inasmuch as they provide additional comparative information about the characteristics of the observed distributions. The parameter α provides an estimate of the shape of each distribution, while β is a scaling parameter. One can assess how the data sets differ with respect to these parameters by determining the large sample 95% confidence intervals (CI) for the difference between the parameters. For example, the difference between the shape parameters from two independent distributions is given by

$$95\% \text{ CI} = (\alpha_1 - \alpha_2) \pm 1.96 \sqrt{\left(\frac{n_1}{n_2}\right) \sigma_1^2 + \left(\frac{n_2}{n_1}\right) \sigma_2^2},$$

Table I. Statistical Estimates and Confidence Intervals for Vasopressin mRNA

Statistic	Definition	Control (\pm SE)	1 day (\pm SE)	95% confidence interval for the difference ^a
α	“Shape” parameter	7.937 \pm 0.706	7.519 \pm 0.611	(-1.403, 2.239)
β	“Scale” parameter	15.06 \pm 1.38	18.79 \pm 1.58	(-7.90, 0.44)
$\alpha\beta$	Mean pixel number per cell	119.52 \pm 2.62	141.28 \pm 2.93	(-29.58, -13.94)*
$\alpha\beta(\beta + 1)$	Variance in pixel numbers	1919.2 \pm 179.7	2795.7 \pm 243.7	(-1486.7, -266.4)*
$\sqrt{(1 + \beta)/\alpha\beta}$	Coefficient of variation	0.3665 \pm 0.0153	0.3743 \pm 0.0144	(-0.0490, 0.0336)

^a A 95% confidence interval on the difference between the control and the 1-day treatments. If this interval contains zero, there is no significant difference at the 5% probability level.

* Difference between control and 1-day treatments is significant at the 5% probability level.

where the subscripts 1 and 2 refer to data obtained from the control and 1-day salt-loaded conditions, respectively, and σ^2 represents the estimated variance (diagonal element of the variance-covariance matrix). CI's for the β parameters are calculated in a similar manner. The confidence interval will subsume zero if there is no significant difference at the 5% probability level between the two groups with respect to the parameter of interest. As illustrated in Table I, the parameter β , for the data of the control and 1-day salt drinking conditions for measures of vasopressin mRNA, falls short of statistical significance ($P = 0.08$), while in Table II the β 's from the oxytocin mRNA measures were different. In both experiments, the α parameters were not statistically different (Tables I and II). This implies that the alteration, relative to control, in the distribution of pixel counts from 1 day of experimental salt treatment is a result of a change in scale (β) rather than in shape (α ; see Discussion).

Several functions of α and β also provide information concerning the data sets (see Tables I and II). First, the means are estimates of central tendency and

Table II. Statistical Estimates and Confidence Intervals for Oxytocin mRNA

Statistic	Definition	Control (\pm SE)	1 day (\pm SE)	95% confidence interval for the difference ^a
α	“Shape” parameter	8.449 \pm 0.801	8.334 \pm 0.726	(-2.000, 2.227)
β	“Scale” parameter	14.71 \pm 1.43	20.15 \pm 1.81	(-10.05, -0.84)*
$\alpha\beta$	Mean pixel number per cell	124.28 \pm 2.80	167.97 \pm 3.54	(-52.71, -34.67)*
$\alpha\beta(\beta + 1)$	Variance in pixel numbers	1952.5 \pm 193.1	3553.3 \pm 329.1	(-2374.8, -826.8)*
$\sqrt{(1 + \beta)/\alpha\beta}$	Coefficient of variation	0.3556 \pm 0.0158	0.3549 \pm 0.0147	(-0.0390, 0.0404)

^a A 95% confidence interval on the difference between the control and the 1-day treatments. If this interval contains zero, there is no significant difference at the 5% probability level.

* Difference between control and 1-day treatments is significant at the probability level.

reflect what is visually evident in the histograms (Fig. 1) and quantile plots (Figs. 2 and 3); *viz.*, there is a significant increase in average pixels per cell as a result of the osmotic stimulation. Second, it is notable that the calculated variance of each distribution is much greater than the calculated mean. In each case this inequality supports the view that the data are not the result of a homogeneous Poisson process, where the mean and variance are equal. Finally, the coefficients of variation are nearly equal and not significantly different (Tables I and II). This observation supports what is observed from visual inspection of the residual quantile plots (Figs. 2 and 3) and affirms what can be inferred from the fact that α is not significantly different in either data set: the differences between the observed data sets is a matter of scale. In fact, for large values of β , $(1 + \beta)/\beta \approx 1$ and the coefficient of variation depends on α only; this illustrates α 's role as a measure of "shape" rather than "scale."

DISCUSSION

Quantitative techniques are a powerful adjuvant for analysis and interpretation of complex data derived from *in situ* hybridization. Statistical analysis, as illustrated here, allows one to remain cognizant of the morphological and dynamic nature of the data source: it permits one to test a probabilistic model and to investigate the critical elements that underlie observed changes. Quantile plotting, as one instance of graphical analysis, is an exploratory and complementary procedure for complex data analysis. It naturally takes advantage of the fact that the investigator's visual system can easily perceive underlying patterns and associations that may not be evident either by inspection of the raw data or from interpretation of single statistical values such as the sample mean (Chambers *et al.*, 1983; Tukey, 1977).

The residual quantile plots directly illustrated the nature of the changes in vasopressin or oxytocin mRNA content per cell profile after rats drink salt water (Figs. 2d and 3d). Had this stimulus caused each cell to exhibit an equal increment in the amount of vasopressin or oxytocin mRNA, a slope of about zero (with y intercept equal to the average increment) would be evident. The magnitude of the differences between data obtained from the rats drinking tap water and data from rats ingesting salt water was a linear function, with the slope of the residual plots greater than zero. This suggests that each cell exhibited a proportional increase in vasopressin or oxytocin mRNA content from osmotic stimulation. That such a biological unity is a property of this neural system was supported by the statistical analysis. As observed, a proportional increment in mRNA content had no impact upon the coefficients of variation (Tables I and II).

Maximum-likelihood estimates were congruent with the notion that the negative binomial probability distribution is an appropriate model for describing grain variation of cell profiles across a defined neuronal system (Fig. 4). We have outlined previously the rationale for this idea (McCabe *et al.*, 1989), where variation over labeled cells is the product of the effects of random isotope disintegration (a Poisson process) plus variation that arises from the fact that each

cell is an independently sampled entity. The model does not take into consideration that the data are obtained from cell profiles and what relationship this actually has to cell profile variation, or to the mRNA content of entire cells. For estimation of cell mRNA content, we have assumed that a relationship does exist and that this approach may be a "robust" quantitative autoradiographic procedure (McCabe *et al.*, 1986b); *viz.*, tissue from different experimental treatments can be legitimately compared. These limitations can be defined only by further work.

In summary, a well-known biological response to maintenance on salt water, which results in an increase in vasopressin and oxytocin mRNA in the cells of the hypothalamoneurohypophysial system, was used as a test system for quantitative *in situ* hybridization. Following *in situ* hybridization, subregions of the supraoptic nucleus were analyzed for either vasopressin or oxytocin mRNA. As evident in Figs. 1–4, increases in the cellular content of both of these mRNA transcripts were observed as a result of salt-water drinking. Graphical analysis was then complemented by statistical estimation and hypothesis testing. Both procedures can increase our understanding of the complex changes in gene expression that occur under *in vivo* conditions.

ACKNOWLEDGMENTS

We thank an anonymous reviewer for helpful comments. The data analysis and preparation of the manuscript were supported in part by NIH Grants NS25913 to J.T.M. and HD05751 to D.W.P. R.A.D. was supported by a Creative Leave Award from the California State University.

REFERENCES

- Chambers, J. M., Cleveland, W. S., Kleiner, B., and Tukey, P. A. (1983). *Graphical Methods for Data Analysis*, Wadsworth, Belmont, CA.
- Defendini, R., and Zimmerman, E. A. (1978). The magnocellular neuro-secretory system of the mammalian hypothalamus. In *The Hypothalamus* (S. Reichlin, R. J. Baldessarini, and J. B. Martin, Eds.), Raven Press, New York, pp. 137–152.
- England, J. M., and Rogers, A. W. (1970). The statistical analysis of autoradiographs. I. Grain count distributions over uniformly labelled sources. *J. Microsc.* **92**:159–165.
- Hou-Yu, A., Lamme, A. T., Zimmerman, E. A., and Silverman, A.-J. (1986). Comparative distribution of vasopressin and oxytocin neurons in the rat brain using a double-label procedure. *Neuroendocrinology* **44**:235–246.
- Hyodo, S., Fujiwara, M., Sato, M., and Urano, A. (1988). Molecular- and immuno-histochemical study on expression of vasopressin and oxytocin genes following sodium loading. *Zoo. Sci.* **5**:1033–1042.
- Ivell, R., and Richter, D. (1984). Structure and comparison of the oxytocin and vasopressin genes from rat. *Proc. Natl. Acad. Sci. USA* **81**:2006–2010.
- Kawata, M. (1983). Immunohistochemistry of oxytocin and vasopressin neurons in dog and rat under normal and experimental conditions. In *Structure and Function of Peptidergic and Aminergic Neurons* (Y. Sano, Y. Ibata, and E. A. Zimmerman, Eds.), JSSP-VNU Science Press, Tokyo, pp. 33–53.
- Kawata, M., McCabe, J. T., Harrington, C., Chikaraishi, D., and Pfaff, D. W. (1988a). *In situ* hybridization analysis of osmotic stimulus-induced changes in ribosomal RNA in rat supraoptic nucleus. *J. Comp. Neurol.* **270**:528–536.

- Kawata, M., McCabe, J. T., and Pfaff, D. W. (1988b). *In situ* hybridization histochemistry with oxytocin synthetic oligonucleotide: Strategy for making the probe and its application. *Brain Res. Bull.* **20**:693–697.
- Kawata, M., McCabe, J. T., Pfaff, D. W., and Sano, Y. (1988c). Gene expression for posterior pituitary hormones studied by *in situ* hybridization histochemistry. In *Recent Progress in Posterior Pituitary Hormones 1988* (S. Yoshida and L. Share, Eds.), Elsevier Science, Amsterdam, pp. 249–255.
- Kendall, M., and Stuart, A. (1977). *The Advanced Theory of Statistics, Vol. 1*, 4th ed., Griffin, London.
- Lewis, M. E., Rogers, W. T., Krause, R. G., II, and Schwaber, J. S. (1989). Quantitation and digital representation of *in situ* hybridization histochemistry. *Met. Enzymol.* **168**:808–821.
- Lightman, S. L., and Young, W. S., III (1987). Vasopressin, oxytocin, dynorphin, enkephalin and corticotrophin-releasing factor mRNA stimulation in the rat. *J. Physiol.* **394**:23–39.
- McCabe, J. T., and Pfaff, D. W. (1989). *In situ* hybridization: A methodological guide. *Meth. Neurosci.* **1**:98–126.
- McCabe, J. T., Morrell, J. I., Ivell, R., Schmale, H., Richter, D., and Pfaff, D. W. (1986a). *In situ* hybridization to localize rRNA and mRNA in mammalian neurons. *J. Histochem. Cytochem.* **34**:45–50.
- McCabe, J. T., Morrell, J. I., and Pfaff, D. W. (1986b). *In situ* hybridization as a quantitative autoradiographic method: An example from vasopressin and oxytocin gene transcription in the Brattleboro rat. In *In Situ Hybridization in Brain* (G. R. Uhl, Ed.), Plenum Press, New York, pp. 73–95.
- McCabe, J. T., Morrell, J. I., and Pfaff, D. W. (1986c). Measurement of vasopressin and oxytocin genes in single neurons by *in situ* hybridization. In *Neuroendocrine Molecular Biology* (G. Fink, A. J. Harmar, and K. W. McKerns, Eds.), Plenum Press, New York, pp. 219–229.
- McCabe, J. T., Desharnais, R. A., and Pfaff, D. W. (1989). Graphical and statistical approaches to data analysis for *in situ* hybridization. *Meth. Enzymol.* **168**:822–848.
- Przybylski, R. J. (1970). Principles of quantitative autoradiography. In *Introduction to Quantitative Cytochemistry—II* (G. L. Wied and G. F. Bahr, Eds.), Academic Press, New York, pp. 477–505.
- Rhodes, C. H., Morrell, J. I., and Pfaff, D. W. (1981). Immunohistochemical analysis of magnocellular elements in rat hypothalamus: Distribution and numbers of neurophysin, oxytocin and vasopressin containing cells. *J. Comp. Neurol.* **198**:45–64.
- Schmale, H., Ivell, R., Briendl, M., Darmer, D., and Richter, D. (1984). The mutant vasopressin gene from diabetes insipidus (Brattleboro) rats is transcribed but the message is not efficiently translated. *EMBO J.* **3**:3289–3293.
- Sherman, T. G., McKelvey, J. F., and Watson, S. J. (1986). Vasopressin mRNA regulation in individual hypothalamic nuclei: A Northern and *in situ* hybridization analysis. *J. Neurosci.* **6**:1685–1694.
- Takamatsu, T., Kitamura, T., and Fujita, S. (1986). Quantitative fluorescence image analysis. *Acta Histochem. Cytochem.* **19**:61–71.
- Tukey, J. W. (1977). *Exploratory Data Analysis*, Addison-Wesley, Reading, MA.
- Uhl, G. R. (1989). *In situ* hybridization: Quantitation using radiolabeled hybridization probes. *Meth. Enzymol.* **168**:741–752.
- Vandesande, F., and Dierickx, K. (1975). Identification of the vasopressin producing and oxytocin producing neurons in the hypothalamic magnocellular neurosecretory system of the rat. *Cell Tissue Res.* **164**:153–162.
- Van Tol, H. H. M., Voorhuis, D. Th. A. M., and Burbach, J. P. H. (1987). Oxytocin gene expression in discrete hypothalamic magnocellular cell groups is stimulated by prolonged salt loading. *Endocrinology* **120**:71–76.
- Wilks, M. B., and Gnanadesikan, R. (1968). Probability plotting methods for the analysis of data. *Biometrika* **55**:1–17.
- Young, W. S., III (1989). *In situ* hybridization histochemical detection of neuropeptide mRNAs using DNA and RNA probes. *Meth. Enzymol.* **168**:702–710.